ISSN 1330-3651 (Print), ISSN 1848-6339 (Online)
https://doi.org/10.17559/TV-20230611000719
Original scientific paper

Efficiency Analysis of Regenerative Brake System Using Flywheel Energy Storage Technology in Electric Vehicles

Zeyneb Nuriye KURTULMUŞ*, Abdulhakim KARAKAYA

Abstract: The increase in fossil fuel consumption used in conventional vehicles has adversely affected carbon emissions in the atmosphere. Due to this negativity, many problems such as global warming, noise pollution, and cost have emerged. To find solutions to these problems, many studies have been conducted to increase the energy storage capacity of Electric Vehicles (EVs) since 1835. EVs produced as a result of these studies work more efficiently than traditional vehicles. However, the driving range problem and charging time are the biggest disadvantages of these vehicles. These disadvantages are a major obstacle for EVs to replace traditional vehicles. In this study, an experimental study was conducted on flywheel-battery in-vehicle topologies, which are recommended to increase the range of EVs and hybrid electric vehicles. In this application, two flywheels with the same rotor radius and different masses were used. Energy was produced by the generator through these flywheels. This energy was employed to charge the batteries. The stored energy and power amounts were investigated depending on the variation in the moment of inertia of both flywheels at the maximum and minimum levels. Because of this examination, it has been determined which flywheels with the same rotor radius but different masses are more suitable for EVs.

Keywords: electric vehicle; energy storage; flywheel-battery; regenerative braking system

1 INTRODUCTION

With the rapid increase in population in the modern world, the need for transportation technologies has increased at this rate. Unfortunately, although transportation options make our lives easier, environmental harm has also grown. Global warming is caused by greenhouse gases and CO_2 emissions emitted into the atmosphere. Because of the Paris Agreement to stop global warming, CO_2 emissions have been reduced and the temperature of the planet has been controlled [1]. Especially in the automotive industry, there is a great trend to producevehicles with as low CO_2 emissions as possible. Major investors have invested heavily in the development of hybrid propulsion vehicles, fuel cell-powered vehicles, and EVs [2]. EVs have advantages such as less exhaust emissions and less noise pollution. However, EVs have disadvantages such as range problems, long charging times, and additional production costs, and advantages over traditional vehicles. For this, various R&D studies are conducted and a new solution is sought every day. To solve the range problem experienced in EVs and hybrid electric vehicles (HEVs), it aims to overcome these problems by increasing the efficiency of the energy storage systems (ESSs) used in vehicles or by developing new methods. For instance, Barmaki et al. investigated a traditional HEV structure. They observed that an HEV contains an internal combustion engine and a fuel tank, and an electric motor and an ESS (battery). In summary, they stated that in an HEV, they used two drivers for the powertrain [3]. In conventional vehicles, kinetic energy is lost as heat energy in the lining in the case of sudden braking or downhill idling. This lost energy is stored in the flywheel system to find a solution to the range problem and shorten the charging time. Various ESSs are suitable for use in regenerative braking systems. One of these, the flywheel energy storage system (FESS), is a mechanism that can store kinetic energy during braking. The ultracapacitor is one of the most widely used devices in regenerative braking systems. When a good material is used in the flywheel system, energy efficiency increases, and a low-cost solution is provided [4]. Doucette and McCulloch compared flywheels, ultracapacitors, and batteries, which are energy storage devices. As a result, they emphasized that flywheels can compete with batteries and ultra capacitors in terms of cost and fuel economy [5]. Faraji et al. They conducted a study on flywheels and observed that high-speed flywheels of 100000 rpm and above have great energy storage potential. [6]. Using a flywheel in the regenerative braking system of a bus in Tehran, the obtained energy was stored. In this study, it was determined that the fuel consumption of the bus decreased by 30% [7]. Volvo tested the flywheel kinetic energy recovery system in its vehicles in 2013. As a result, it was shown that the flywheel system could reduce fuel consumption by 25% [8]. The flywheel system developed by Siemens for EVs has both met the high specific power demand and improved energy use [9]. FESSs have been integrated into 500 buses in London since they began to be commercially produced. In this application, it was concluded that 20% fuel saving was achieved [10]. FESSs are not only suitable for EVs and HEVs but also for rail transport. Thanks to 2.9 kWh, 725 kW FESS, it is possible to increase energy efficiency by up to 31% and achieve cost savings of up to 11% [11]. The in-vehicle flywheel-battery topologies that have been for usage in EVs and HEVs to enhance range are considered in this research. Two flywheels were used, each with a different moment of inertia but the same rotor radius. Flywheels with kinetic energy were used to generate electricity via generators. The generated energy was used to charge the battery. The investigation of the moment of inertia, angular velocity variations, and energy storage efficiency of two flywheels operating under the same circumstances and with different masses resulted in this working difference. The prototype experimental setup was used to obtain the values used in the analysis. In addition, the flywheels' lowest and highest energy capacities were compared.

2 GENERAL FEATURES OF THE FLYWHEELS

Flywheels are an excellent energy storage device model because of their low maintenance costs, long life, high efficiency, being away from the effect of the current depth, being environmentally friendly, having a wide operating temperature range, and at the same time survival rugged equipment [12-15]. The energy that provides the rotation in the flywheel is obtained from an external source, and the storage process is performed [16]. FESSs can rotate at high speeds of up to approximately 50000 rpm [17-18]. To achieve a higher energy capacity, FESSs either contain a rotor with a significant moment of inertia or operate at a high rotational speed. The flywheels are cylindrical with enough space to fit a shaft. Therefore, the mass-momentum of inertia of the hollow cylinder is obtained as in Eq. (1).

$$I = \frac{1}{2} m \left({r_{\text{out}}}^2 + {r_{\text{in}}}^2 \right) \tag{1}$$

In Eq. (1), m is the mass (kg), r_{out} is the flywheel outer radius (m), and r_{in} represents the flywheel inner radius (m).

The components of flywheel rotors are made of composite or metallic materials [19]. However, if they are used in vehicles, they must be able to withstand forces from different directions, and for this, the classic ship-ship structure is preferred. The bearings selected here are made of special alloys and can withstand very high static and dynamic forces [20]. A motor/generator directly connected to the flywheel rotor is used to consume and recharge energy. A bidirectional converter is connected to the motor/generator. The flywheel rotor is a critical element because it stores energy at high speeds. The design and power of this rotor are important issues. While steel-based rotors were initially used in flywheel designs composite-based rotors were later used [21]. To increase the energy density of flywheels and reduce their costs, research is still ongoing in which materials such as glass fiber and carbon composite are used in flywheels [16]. Eq. (2) shows that the energy storage capacity of the flywheel increases with the square of the rotor speed and the momentum of inertia [22]. The bearing system is improved, allowing the rotor to reach higher speeds. Thus, idling losses are reduced and the life of the system is extended up to approximately 25 years. FESS stands out as a technology with a very high power density. With the rotor weighing 277 kg and 20000 rpm, 350 kW nominal and 5 MW peak power can be obtained [23]. In this case, the power density is equal to 1.26 kW/kg and the peak value is 18 kW/kg.

$$E_{flywheel} = \frac{1}{2} I \left({w_{\max}}^2 - {w_{\min}}^2 \right) = E_{load} - E_{motor} \tag{2}$$

In Eq. (2), $E_{flywheel}$ is the energy (Joule) stored by the flywheel (Joule), I is the rotational inertia of FESS (kg m^2), E_{load} is the energy required by the load (Joule), E_{motor} is the energy output of the motor (Joule), $w_{\max}$ and $w_{\min}$ are the maximum and minimum angular velocity of the flywheel $\left(\frac{\text{rad}}{\text{s}} \right)$ [22].

3 WORKING PRINCIPLE OF FLYWHEEL ENERGY STORAGE SYSTEMS IN ELECTRIC VEHICLES

In the prototype designed for this application, no continuously variable transmission (CVT) system was used, but the rotational energy of the engine wheels during recovery was applied to the flywheel through the pulley. Here, the pulley system behaved like a CVT. However, the engine/generator unit was not used either. The experimental set was set up on the basis of the vehicle's recovery system only. In Fig. 1, the alternating current (AC) taken from the network was converted into mechanical energy using a universal motor. Then, this energy was transferred to the flywheel using the pulley system. Thanks to this energy, the flywheel started to charge quickly and reached high rpms. The obtained mechanical energy was then obtained because of the brushless direct current (BLDC) motor working in the generator mode, AC energy.

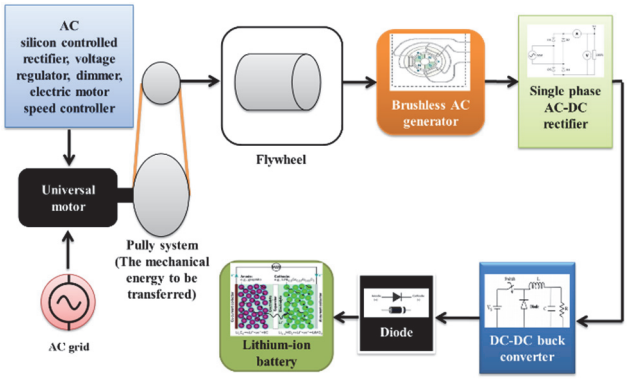

Figure 1 Block diagram of prototype system designed for application

Fig. 2 shows the voltage signal obtained from the generator. This signal was obtained by driving the generator at 5000 rpm. Since batteries can be charged with direct current (DC) voltage, the AC obtained from the generator must be converted to DC. For this, a full-wave AC-DC rectifier is used. The rectified voltage was transferred to the battery via a DC-DC converter.

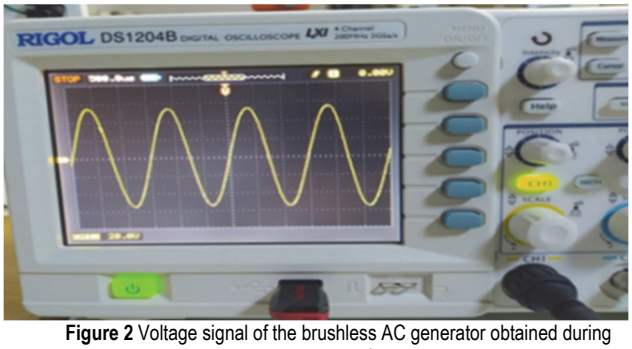

Figure 2 Voltage signal of the brushless AC generator obtained during generator operation

4 MATERIALS USED IN PRACTICE

In this study, the results obtained by comparing 2 flywheels with different masses and lengths but the same radius were examined. Since the number of revolutions affects the angular velocity, the maximum and minimum angular velocity values of the system are obtained using Eq. (3). The energy capacity of the flywheel is proportional

to the square of the angular velocity according to Eq. (2). Therefore, angular velocity is a major factor in energy efficiency.

$$\omega_{rm} = \frac{2\pi n}{60} \tag{3}$$

In Eq. (3), n is the rpm.

4.1 Features of Electric Motors Used in Practice

Although universal motors have disadvantages such as high noise and small electric arcs, they are used in industry and many household appliances because they are cheap, have simple structures, and can be produced in small sizes [24-26]. Because of these advantages, a universal motor was used to drive the flywheel. The minimization of ripples is the most important work in BLDC motors. BLDC motors are preferred in many applications because they have many advantages such as easy speed control, long service life, high efficiency, and high-power density [27-31]. Aviation, the automotive industry, robotics, medical devices, and EVs are examples of applications where the BLDC motor is used [27].

4.2 Features of Flywheels Used in Practice

Fig. 3 and Fig. 4 show pictures of the flywheels used in the application. Fig. 3a and Fig. 4a show 6201RS 12 × 32 × 10 mm high-quality steel bearings and covers mounted on the shaft of the flywheels. Fig. 3b and Fig. 4b show flywheels mounted in a safety sheath against the possibility of rupture, breakage, and fragmentation at high rpm. Tab. 1 shows the physical properties of the flywheels used in the application.

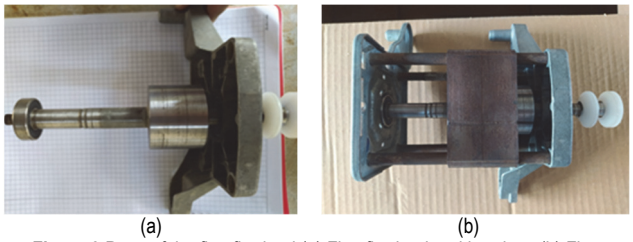

(a) (b)

Figure 3 Parts of the first flywheel (a) First flywheel and bearings (b) First flywheel mounted in the safety cover

(a) (b)

Figure 4 Parts of the second flywheel (a) Second flywheel, bearings, covers, and safety cover (b) Second flywheel mounted in the safety cover

Table 1 Physical properties of flywheels used in practice

Flywheel	Length / mm	Mass / kg	Outer diameter / mm	Inner diameter / mm
First flywheel	40	0.52	49	15
Second flywheel	60.8	0.79	49	15

4.3 Purpose of Use of the Materials in the Experiment Set

Fig. 5 shows the materials used in the experiment set. A voltage regulator power supply is used to prevent the universal motor from being damaged by voltage fluctuations. The revolutions of universal motors can reach very high speeds such as 20000 rpm. In addition, rotation and development moments are high. For this reason, the mechanical energy in the universal engine was softly given to the flywheel using the pulley system.

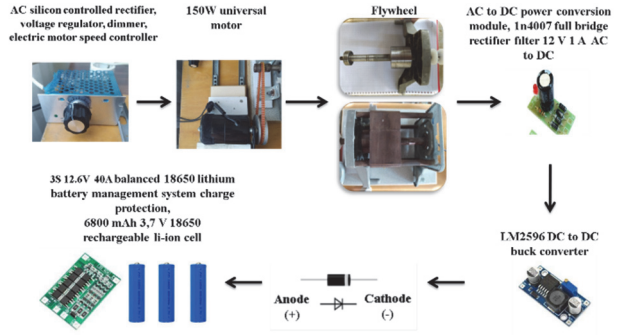

Figure 5 Materials used in the experimental set

In Fig. 6, the brushless AC, which is coupled with the flywheel system, was operated as a generator and electrical energy was produced. The obtained one-phase voltage was rectified and transferred to the battery. The voltage, current, and power values at the step-down rectifier output were recorded using Arduino and an Adafruit INA-219 board. The 6800 mAhLi-Ion battery used in the system was charged in a controlled manner with the 3S 40A lithium battery management system.

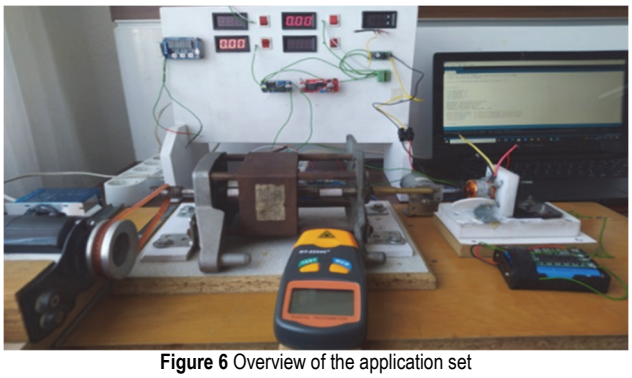

Figure 6 Overview of the application set

5 EXPERIMENT RESULTS

5.1 Test Results According to the Change in the Momentum of Inertia

The cycle-time graph obtained in the study with the first flywheel is shown in Fig. 7. The flywheel was charged for 84 seconds. According to the values obtained, the maximum efficiency was reached at 21993 rpm. The flywheel was maintained at this level for 11 s, and then unloaded and brought to the discharge position. The purpose here is to store the potential energy of the vehicle when braking or going downhill. Under normal conditions, braking should be held for less than 1 min. However, in this study, the idle operation of the vehicle was also considered.

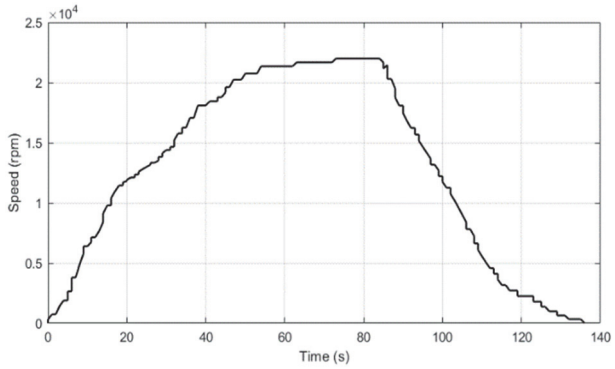

Figure 7 Speed-time graph of the first flywheel

The cycle-time graph obtained in the study using the second flywheel is shown in Fig. 8. The flywheel was charged for 79 s. In the experiment with a second flywheel with more mass, the maximum efficiency was reached at 19425 rpm. The flywheel, which was held at this speed for 4 s, then decreased to 19186 rpm. At this level, it is held for 6 s. Afterwards, the flywheel was brought to the discharge position by removing it.

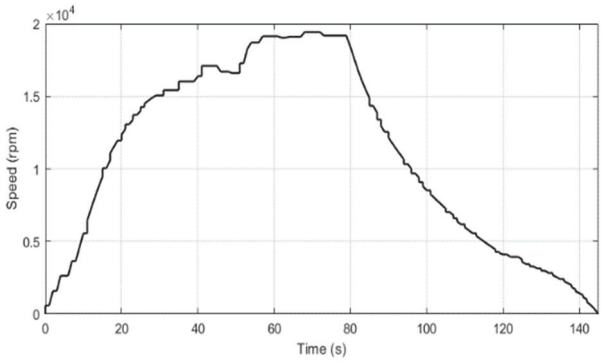

Figure 8 Speed-time graph of the second flywheel

The cutting speed indicated in Tab. 2 represents the speed at which the energy obtained from the flywheel ends. This level resulted in 3931 and 2244 rpm for the second and first flywheel systems, respectively. Since the mass of the first flywheel system is less than that of the second flywheel system, the number of revolutions is higher.

Table 2 Speed changes in flywheel systems

Speed	Second flywheel system speed change / rpm	First flywheel system speed change / rpm
Maximum	19425	21993
At power off	3931	2244

In order for the battery used in the experiment to be charged efficiently, the required charge voltage must be greater than the battery voltage. For this reason, the battery started to charge between 11.1 and 12.6 V. In Fig. 9, a voltage of 13.1 V was obtained at 21993 rpm. At 2244 rpm, the voltage obtained from the generator is cut off. At 2244 rpm, the voltage from the generator is cut off. At 14387 rpm, the lithium-ion battery's necessary charging voltage of 11.1 V was attained (in the thirtieth second). When the flywheel was driven, it fed the battery for 54 s. When it was not driven, it fed the battery for 9 s. Battery supply stopped because the generator voltage dropped to 10.9 V at 14640 rpm (at 95 s). The flywheel provided energy to the battery for 63 s, both when it was driven and when it was not.

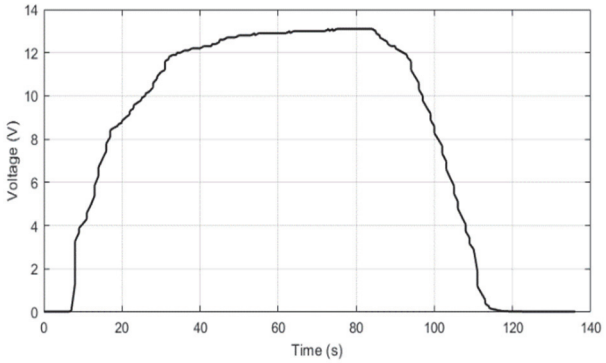

Figure 9 Voltage-time graph of the first flywheel

In Fig. 10, 12.7 V was obtained from the generator at 19425 rpm. At 3931 rpm, the voltage obtained from the generator was cut off. The battery started to be fed with a voltage of 11.1 V obtained at 14262 rpm (in the twenty-fifth second). The maximum value of 12.6 V required for the battery was reached in 56 s (at 19134 rpm). When the flywheel was driven, it fed the battery for 54 s. If it was not driven, it fed the battery for 5 s. Because the generator voltage dropped to 10.85 V at 14344 rpm (the 85th second), the battery supply stopped. The flywheel provided energy to the battery for 59 s, both when it was driven and when it was not.

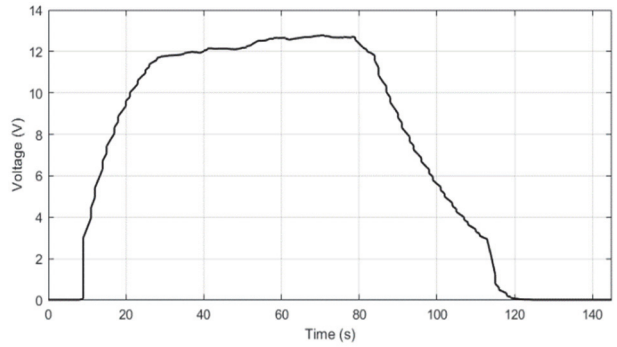

Figure 10 Voltage-time graph of the second flywheel

Fig. 11 shows the current-time graph of the first flywheel. After 30 s, the battery started to charge. After about 50 s, the charging current varied between 600 and 725 mA. At the sixty-ninth second, a maximum current of 725 mA was recorded.

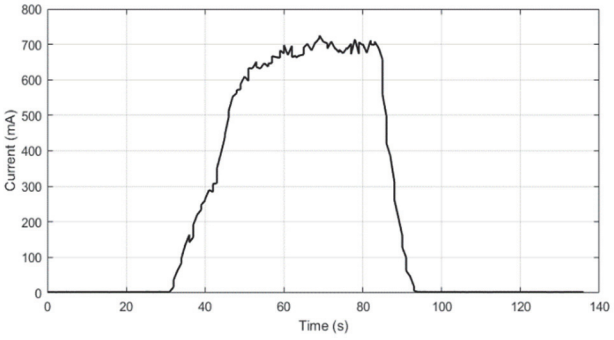

Figure 11 Current-time graph of the first flywheel

The second flywheel's current-time graph is shown in Fig. 12. In the seventieth second, a maximum current of 565 mA was recorded. The charging currents continued between 2.4 and 2.6 mA after falling below 2.8 mA in both flywheels.

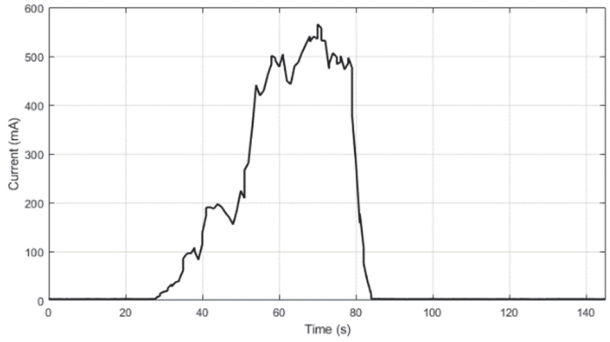

Figure 12 Current-time graph of the second flywheel

The maximum power in Fig. 13 was achieved in the sixty-ninth second. These values are equivalent to 9425 mW at 13 v and 725 mA. The maximum power in Fig. 14 was attained at the seventieth second. These values correspond to 7230 mW at 12.7 V and 565 mA.

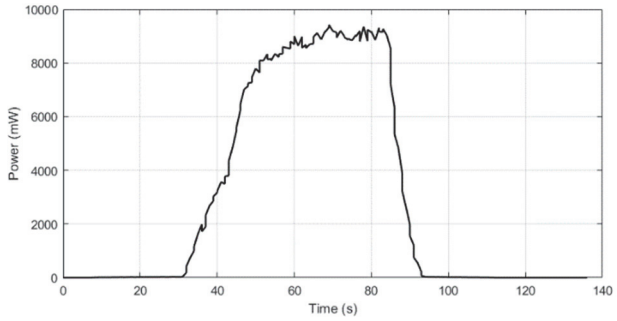

Figure 13 Power-time graph of the first flywheel

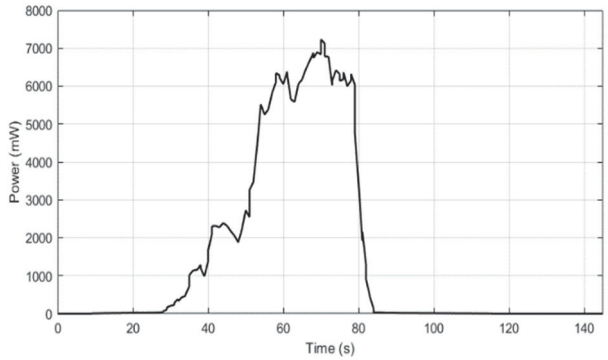

Figure 14 Power-time graph of the second flywheel

5.2 Energy Efficiency of the Flywheels

A total of three experiments were conducted for each flywheel under the same conditions. The data obtained from the experiments are presented in Tab. 3. In Tab. 3, the optimum energy amounts obtained for the two flywheels are obtained on the basis of Eq. (2). Because the inertia momentum of the first flywheel is low, its speed is high.

The square of the angular velocity in the second flywheel was lower than that in the first flywheel. However, it has been determined that the energy of the second flywheel is higher than that of the first flywheel. This is because the mass in Eq. (3) affects the momentum of the inertia.

Table 3 Test result angular velocity-energy amounts for the first and second flywheels

First Flywheel (Low Momentum of Inertia)		
$\left(w_{max}{}^2 - w_{min}{}^2\right)$ rad^2/s^2	I / kg m^2	E / J
4058213.20	0.00017069	8.77
4660236.39		10.07
5249056.03		11.35
Second Flywheel (High Momentum of Inertia)		
3462562.03	0.000259318	11.37
3496705.565		11.48
3968434.844		13.03

Eq. (4) was used to compare the flywheels' energy efficiency at their maximum and minimum points. Eq. (5) was used to compare the flywheel power efficiencies at their maximum and minimum points. Tab. 4 shows the obtained values. Tab. 4 shows that the second flywheel has minimum and maximum energy levels that are, respectively, 23% and 13% higher than those of the first flywheel. However, it has been shown that the first flywheel has 3% and 23% more power, respectively, than the second flywheel, when the minimum and maximum power quantities generated from the flywheels are evaluated.

$$\eta_{energy} = \frac{E_2 - E_1}{E_2} \tag{4}$$

$$\eta_{power} = \frac{P_1 - P_2}{P_1} \tag{5}$$

In Eq. (4), E_1 is the amount of energy obtained from the first flywheel (J), E_2 is the amount of energy obtained from the second flywheel (J). In Eq. (5), P_1 is the amount of power obtained from the first flywheel (mW) and P_2 is the amount of power obtained from the second flywheel (mW).

Table 4 Energy and power efficiency values obtained from flywheels

The amount of energy obtained from the flywheels / J	η_{min}	η_{max}
E_1	8.77	11.37
E_2	11.35	13.03
Efficiency	23%	13%
Amount of power obtained from the flywheels (mW)	η_{min}	η_{max}
P_1	30.24	9425
P_2	29,295	7230
Efficiency	3%	23%

6 CONCLUSION

In this study, the flywheel system is used to store the energy obtained from the HEV and EV for regenerative braking or downhill vehicle in the battery. The focus is on the momentum of inertia in the energy storage formula of the flywheels. To achieve this, two flywheels with different masses and the same rotor radius were employed. The advantages and disadvantages of these two flywheels were compared. Using the designed prototype, the difference in the squares of the maximum and minimum angular velocities obtained from the two-flywheel system operated under the same conditions and the amounts of energy were compared. Because of this comparison, it was determined

that the maximum and minimum energy amounts obtained from the second flywheel were 23% and 13% higher, respectively, than those obtained from the first flywheel. However, the minimum and maximum power amounts obtained from the flywheels were found to be 3% and 23% higher for the first flywheel than for the second flywheel. In this application, a molecularly lighter and more reliable material can be used instead of steel. In addition, a material that can reach high speeds and is impacts-resistant and breaks is preferred. Because weight is an important factor in the momentum of inertia. In this study, the high inertia momentum is an advantage because the flywheel does not reach high speeds in in-vehicle use. However, it has been determined that the weight is too high and the power obtained from the generator is low. On the other hand, as the flywheel with low inertia momentum can reach higher speeds, the power obtained increases. However, the disadvantage is that the flywheel has low inertia momentum due to the negative effects that may occur due to high speeds and skidding. Therefore, a new study can be conducted on the optimum weight and diameter of flywheels used in EVs.

7 REFERENCES

[1] Saerbeck, B., Well, M., Jörgens, H., Goritz, A., & Kolleck, N. (2020). Brokering climate action: The UNFCCC secretariat between parties and nonparty stakeholders. *Global Environmental Politics*, *20*(2), 105-127. https://doi.org/10.1162/glep_a_00556

[2] Gordić, M., Stamenković, D., Popović, V., Muždeka, S., & Mićović, A. (2017). Electric vehicle conversion: Optimisation of parameters in the design process. *Tehnički vjesnik*, *24*(4), 1213-1219. https://doi.org/10.17559/TV-20160613131757

[3] Barmaki, R., Ilkhani, M., & Salehpour, S. (2016). Investigation of energy usage and emissions on plug-in and hybrid electric vehicle. *Tehnicki vjesnik/Technical Gazette*, *23*(3). https://doi.org/10.17559/TV-20140928112417

[4] Pullen, K. R. & Dhand, A. (2014). Mechanical and electrical flywheel hybrid technology to store energy in vehicles. *Alternative fuels and advanced vehicle technologies for improved environmental performance*, 476-504. https://doi.org/10.1533/9780857097422.2.476

[5] Doucette, R. T. & McCulloch, M. D. (2011). A comparison of high-speed flywheels, batteries, and ultracapacitors on the bases of cost and fuel economy as the energy storage system in a fuel cell based hybrid electric vehicle. *Journal of Power Sources*, *196*(3), 1163-1170. https://doi.org/10.1016/j.jpowsour.2010.08.100

[6] Faraji, F., Majazi, A., & Al-Haddad, K. (2017). A comprehensive review of flywheel energy storage system technology. *Renewable and Sustainable Energy Reviews*, *67*, 477-490. https://doi.org/10.1016/j.rser.2016.09.060

[7] Esfahanian, M., Safaei, A., Nehzati, H., Esfahanian, V., & Tehrani, M. M. (2014). Matlab-based modeling, simulation and design package for eletric, hydraulic and flywheel hybrid powertrains of a city bus. *International Journal of Automotive Technology*, *15*, 1001-1013. https://doi.org/10.1007/s12239-014-0105-8

[8] Li, H., Chu, J., & Sun, S. (2022). Development of a Flywheel Hybrid Power System in Vehicles without the Electric Drive Device Rated Capacity Limit. *World Electric Vehicle Journal*, *13*(2), 27. https://doi.org/10.3390/wevj13020027

[9] Hu, K. W. & Liaw, C. M. (2013). On the flywheel/battery hybrid energy storage system for DC microgrid. *2013 1st International Future Energy Electronics Conference (IFEEC)*, Tainan, Taiwan, 119-125. https://doi.org/10.1109/IFEEC.2013.6687490

[10] Erhan, K. & Özdemir, E. (2021). Prototype production and comparative analysis of high-speed flywheel energy storage systems during regenerative braking in hybrid and electric vehicles. *Journal of Energy Storage*, *43*, 103237. https://doi.org/10.1016/j.est.2021.103237

[11] Rupp, A., Baier, H., Mertiny, P., & Secanell, M. (2016). Analysis of a flywheel energy storage system for light rail transit. *Energy*, *107*, 625-638. https://doi.org/10.1016/j.energy.2016.04.051

[12] Kohari, Z. & Vajda, I. (2005). Losses of flywheel energy storages and joint operation with solar cells. *Journal of materials processing technology*, *161*(1-2), 62-65. https://doi.org/10.1016/j.jmatprotec.2004.07.057

[13] Truong, L., Wolff, F., Dravid, N., & Li, P. (2000). Simulation of the interaction between flywheel energy storage and battery energy storage on the international space station. *Collection of Technical Papers. 35th Intersociety Energy Conversion Engineering Conference and Exhibit (IECEC)*, Las Vegas, NV, USA, 848-854. https://doi.org/10.1109/IECEC.2000.870883

[14] Pieronek, T. J., Decker, D. K., & Spector, V. A. (1997). Spacecraft flywheel systems-benefits, and issues. *Proceedings of the IEEE 1997 National Aerospace and Electronics Conference*, Dayton, OH, USA, 589-593 https://doi.org/10.1109/NAECON.1997.622703

[15] Ries, G. & Neumueller, H. W. (2001). Comparison of energy storage in flywheels and SMES. *Physica C: Superconductivity*, *357*, 1306-1310. https://doi.org/10.1016/S0921-4534(01)00484-1

[16] Ofak, Z., Župan, A., & Plavšić, T. (2019). Transmission grid connection of energy storage facilities-overview and challenges. *Tehnički vjesnik*, *26*(3), 862-871. https://doi.org/10.17559/TV-20180216125257

[17] Brockbank, C. (2009). Application of a variable drive to supercharger & turbo compounder applications. *SAE Technical Paper*, *8*. https://doi.org/10.4271/2009-01-1465

[18] Brockbank, C. & Greenwood, C. (2010). Fuel economy benefits of a flywheel &CVT based mechanical hybrid for city bus and commercial vehicle applications. *SAE International Journal of Commercial Vehicles*, *2*(2), 115-122. https://doi.org/10.4271/2009-01-2868

[19] Li, X. & Palazzolo, A. (2022). A review of flywheel energy storage systems: state of the art and opportunities. *Journal of Energy Storage*, *46*, 103576. https://doi.org/10.1016/j.est.2021.103576

[20] Šonský, J. & Tesař, V. (2019). Design of a stabilised flywheel unit for efficient energy storage. *Journal of Energy Storage*, *24*, 100765. https://doi.org/10.1016/j.est.2019.100765

[21] Erdemir, D. & Dincer, I. (2020). Assessment of renewable energy-driven and flywheel integrated fast-charging station for electric buses: A case study. *Journal of Energy Storage*, *30*, 101576. https://doi.org/10.1016/j.est.2020.101576

[22] Yan, X., Nie, S., Chen, B., Yin, F., Ji, H., & Ma, Z. (2023). Strategies to improve the energy efficiency of hydraulic power unit with flywheel energy storage system. *Journal of Energy Storage*, *59*, 106515. https://doi.org/10.1016/j.est.2022.106515

[23] Pichot, M. A., Kajs, J. P., Murphy, B. R., Ouroua, A., Rech, B. M., Hayes, R. J., & Palazzolo, A. B. (2001). Active magnetic bearings for energy storage systems for combat vehicles. *EEE transactions on magnetics*, *37*(1), 318-323. https://doi.org/10.1109/20.911846

[24] Oancea, C. D., Petre, V. C., & Boicea, V. A. (2019). Educational and Experimental Study for Evaluation of an Universal Motor. *2019 11th International Symposium on*

Advanced Topics in Electrical Engineering (ATEE), Bucharest, Romania, 1-4. https://doi.org/10.1109/ATEE.2019.8724929

[25] Di Gerlando, A. & Perini, R. (2006). Model of the commutation phenomena in a universal motor. *IEEE Transactions on Energy Conversion*, *21*(1), 27-33. https://doi.org/10.1109/TEC.2004.841514

[26] Di Gerlando, A. & Perini, R. (2013).The universal motor: A classic machine with evergreen challenges in design and modeling. *2013 IEEE Workshop on Electrical Machines Design, Control and Diagnosis (WEMDCD)*, Paris, France, 85-94. https://doi.org/10.1109/WEMDCD.2013.6525168

[27] Chen, X. & Liu, G. (2019). Sensorless optimal commutation steady speed control method for a nonideal back-EMF BLDC motor drive system including buck converter. *IEEE Transactions on Industrial Electronics*, *67*(7), 6147-6157. https://doi.org/10.1109/TIE.2019.2945282

[28] Liu, G., Chen, S., Zheng, S., & Song, X. (2016). Sensorless low-current start-up strategy of 100-kW BLDC motor with small inductance. *IEEE Transactions on Industrial Informatics*, *13*(3), 1131-1140. https://doi.org/10.1109/TII.2016.2607158

[29] Lee, A. C., Fan, C. J., & Chen, G. H. (2017). Current integral method for fine commutation tuning of sensorless brushless DC motor. *IEEE Transactions on Power Electronics*, *32*(12), 9249-9266. https://doi.org/10.1109/TPEL.2017.2652847

[30] Yang, L., Zhu, Z. Q., Bin, H., Zhang, Z., & Gong, L. (2020). Safety operation area of zero-crossing detection-based sensorless high-speed bldc motor drives. *IEEE Transactions on Industry Applications*, *56*(6), 6456-6466. https://doi.org/10.1109/TIA.2020.3012594

[31] Gobinath, S. & Madheswaran, M. (2020). Deep perceptron neural network with fuzzy PID controller for speed control and stability analysis of BLDC motor. *Soft Computing*, *24*, 10161-10180. https://doi.org/10.1007/s00500-019-04532-z

Contact information:

Zeyneb Nuriye KURTULMUŞ, MSc
(Corresponding author)
Department of Energy System Engineering, Faculty of Technology,
Kocaeli 41001, Turkey
E-mail: zeyneppkurtulmuss@gmail.com

Abdulhakim KARAKAYA, Asst Prof.
Department of Energy System Engineering, Faculty of Technology,
Kocaeli 41001, Turkey
E-mail: akarakaya@kocaeli.edu.tr